TUNABLE THERMO-OPTIC FILTER FOR WDM APPLICATIONS

D. Hohlfeld, M. Epmeier, H. Zappe
Laboratory for Micro-optics, Institute for Microsystem Technology, University of Freiburg
Georges-Köhler-Allee 102, 79110 Freiburg, GERMANY

ABSTRACT

In this paper we present a novel MEMS-based concept for tunable optical filters for use in wavelength-division multiplexing (WDM) systems. Such a filter is essential for monitoring and reconfiguration of optical networks. Our device is based on a Fabry-Perot interferometer employing a silicon cavity and silicon-based dielectric Bragg mirrors. It is fabricated as a free-standing membrane. Wavelength tuning is achieved through thermal modulation of the resonator's optical thickness. We present the measurement of optical filter performance and tunability. Numerical simulation results of its steady-state and transient thermal behavior are also given.

INTRODUCTION

Wavelength division multiplexing has become the standard technology in fiber-based long-haul data transmission. As channel number increases there is a growing need for wavelength-monitoring. Furthermore, there is a great demand for network elements allowing fast and flexible reconfiguration of optical networks. Tunable filters are well suited for these functions. Several common approaches for realizing filter tuning mechanisms are known, based on electrostatic, electro-optic or piezoelectric effects. In addition there is a class of Fabry-Perot based micromachined tunable filters which varies the resonator-length through physically adjusting the distance between the mirrors by electrostatic or thermal actuation [1,2]. These elements are challenging to fabricate and fragile during operation. We propose here a solid-state device which is thermally modulated. Advancing the work given in [3] we use a much thinner resonator combined with a micromachined suspension, which results in improved optical and electrical behavior.

OPTICAL FILTER PRINCIPLE

The filter element described in this paper uses an etalon-like structure consisting of a resonator with both sides semi-reflecting. Light entering the filter experiences multiple-beam interference so that a set of evenly spaced wavelengths λ_m is selected:

$$\lambda_m = 2 \cdot n_c \cdot l_c / m \qquad (1)$$

The refractive index of the resonator is given by n_c , its length is l_c and m is an integer. Modulation of the selected wavelengths is achieved through varying the optical thickness $n_c \cdot l_c$. The free spectral range *FSR*, describing the frequency spacing between two neighbouring transmission maxima, is given as:

$$FSR = c / (2 \cdot n_c \cdot l_c) \qquad (2)$$

where c is the speed of light in vacuum. The finesse F of a Fabry-Perot filter is proportional to the reflectivity of its mirrors and the resonator length, so that both have to be increased to improve the finesse. A consequence of using thicker resonators is that the free spectral range decreases. This range has to be broader than the width of the employed transmission band in order to prevent other unwanted signals to be selected.

For further improving the filter performance by narrowing the transmission peaks, highly reflecting mirrors are used. The resonator is surrounded on both sides by dielectric mirrors. These are made of N pairs of two materials with different refractive indices. Each layer has an optical thickness of $\lambda/4$, where λ is the center wavelength. The overall reflectivity increases with N and with the difference in refractive index between both materials.

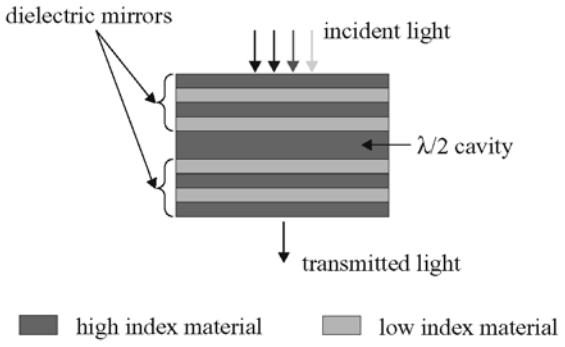

Figure 1. *Schematic setup of a Fabry-Perot filter with a solid-state cavity and dielectric mirrors*

For the concept to be presented, the optical thickness of the resonator is modulated by thermal means. Variations in temperature give rise not only to changes in physical thickness but also alter the refractive index. This is known as the thermo-optic effect, which in this case dominates the filter behavior. Polycrystalline silicon was chosen as the resonator's material, because of its high thermo-optic coefficient.

0-7803-7185-2/02/$10.00 ©2002 IEEE

STRUCTURAL DESIGN

The optical layers are deposited onto a silicon wafer. A thin film heater structure was chosen to realize heating and an additional resistor will be integrated with the heater for temperature sensing and therefore enabling feedback control.

In order to reduce power consumption, the substrate material will be removed from the backside through anisotropically etching a cavity below the filter area as shown in Figure 2. The removal of substrate material also prevents parasitic optical resonances from occuring between the upper filter and the (reflecting) backside of the wafer.

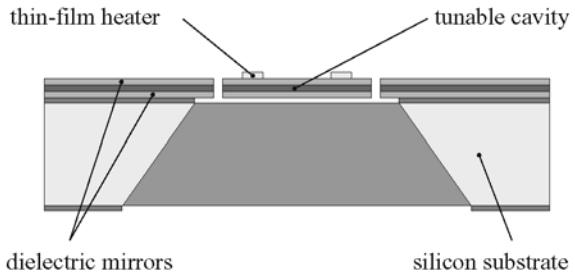

Figure 2. *Cross-section of the filter element (not to scale).*

The thermal isolation of the filter membrane can further be improved through a micromachined suspension. In this case the membrane is fixed to the substrate using cantilever structures, which also support the electrical supply lines. This geometry also eliminates the effects of in-plane mechanical stress such as buckling, since lateral extension of the filter membrane is compensated through bending of the supporting arms. Furthermore there is no warpage expected for the multilayer-structure because of its symmetric structure.

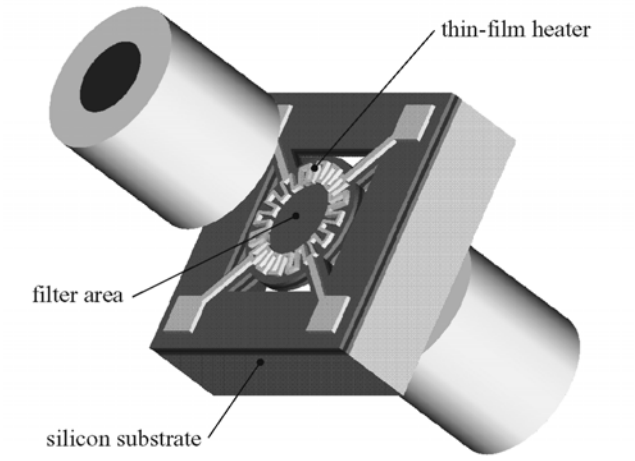

Figure 3. *Model showing the device with the suspended circular filter membrane between two fibers.*

The completed filter is placed between two collimating or focussing devices for realizing transmission operation as is shown in Figure 3.

SIMULATION RESULTS

The main design goals for the optical filter are low power consumption, fast thermal response and high tuning range. The geometry of the thin film heater and the optional suspension structure were optimized using a two-dimensional finite-element model of the multilayer-structure. In this model variations in temperature are restricted to occur within the plane of the filter-layers. The different thermal, electrical and structural properties of the used materials are taken into account by using calculated material properties. These represent the regions where the heater is located on top of the filter structure, the actual filter layers and finally the substrate area. The model was implemented using ANSYS V5.7.

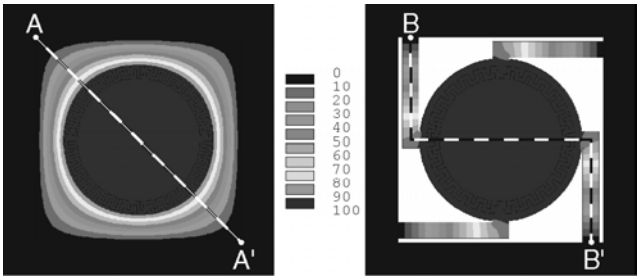

Figure 4. *Temperature distribution within a filter membrane for two different setups (side length of membrane area= 250 μm).*

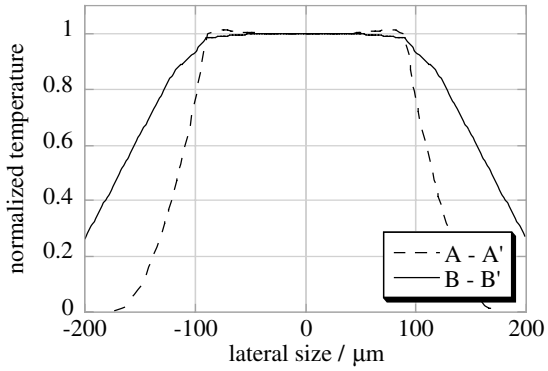

Figure 5. *Temperature curves along the paths given in Figure 4. Temperature varies less than 1 % within a central region of 150 μm diameter.*

As the center area of the filter membrane is used for optical filtering, it is important to assure a homogeneous temperature distribution within this region. Otherwise degradation in optical filter performance will occur, because portions of the incident light beam will see slightly different filter wavelengths. Therefore a circular shape for the filter membrane was chosen. Simulations show that a thermally isolated membrane reaches very homogeneous temperature distributions while temperature gradients occur only in the suspending arms towards the

substrate, as shown in Figure 4 and Figure 5. Relative temperature variations of less than 1 % over the whole filter area can be obtained.

The heating efficiency, i.e. the temperature difference which can be achieved per watt input power, should also be optimized. Values of several 100 K/mW have been shown by simulation to be feasible for isolated membranes. This shows that a temperature difference of 500 K can be obtained by using an electrical input power of only a few milliwatts. Both design goals, i.e. homogeneous temperature distribution and high heating efficiency, are best accomplished using large membranes with a diameter of more than 250 µm.

Table 1. *Heating efficiencies for different membrane sizes. Data refers to fabricated heater designs. (The lateral size defines the dimension of the anisotropically etched cavity.)*

lateral size / µm	heating efficiency / K mW^{-1}	
	without suspension	suspended membrane
100	16.3	159
250	22.2	532
500	13.6	959

Finally, the transient thermal response was simulated. Tunable filters need to adjust the filter wavelength within milliseconds. Heating is accomplished by application of an electrical signal and dissipation of electrical power, whereas cooling takes place through radiative and conductive thermal losses from the membrane. This behavior is dominated by the thermal capacity of the membrane materials and the thermal resistance, which connects membrane and substrate. Figure 6 gives the temperature versus time of the membrane's center.

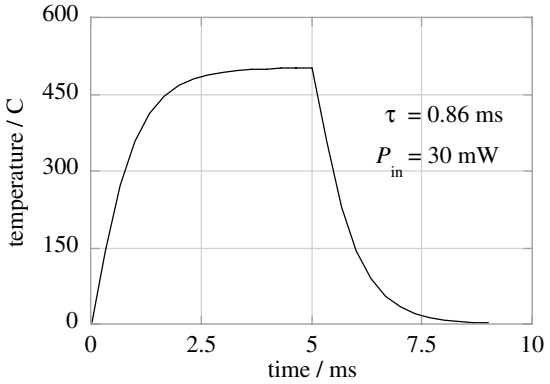

Figure 6. *Simulated transient thermal response of a filter without suspension (membrane side length = 100 µm).*

Thermal systems can be described through first-order-differential equations, so that heating and cooling processes can be approximated by exponential functions. Characteristic time constants obtained by numerical simulation are given in Table 2 for several designs. A higher tuning speed can be reached for small membranes, enabling modulation at several kilohertz. It should be noted that, as a consequence, higher electrical input power is necessary.

Table 2. *Time constants for different membrane configurations*

lateral size / µm	time constants τ / ms	
	without suspension	suspended membrane
100	0.86	3.35
250	5.25	29.6
500	26.5	187

Increasing the membrane size improves heating efficiency and also results in slower thermal response. Therefore a tunable filter of this kind can be optimized either for low power consumption or high tuning speed.

FABRICATION

The present work considers a filter consisting of a silicon etalon cavity surrounded by two Bragg mirrors, initially deposited on a bulk silicon substrate. The film thickness of the cavity is 228 nm, corresponding to an optical thickness of λ/2 at the WDM-relevant wavelength of 1575 nm. The dielectric mirrors consist of two pairs of λ/4-stacks (Figure 7). The high index layers consist of 114 nm thick LPCVD-polycrystalline silicon and the low index layers consist of silicon dioxide deposited by means of PECVD with a thickness of 280 nm.

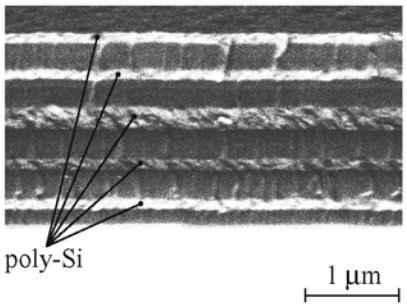

Figure 7. *SEM image of the filter-structure showing the λ/2 cavity embedded between two dielectric Bragg mirrors.*

The final filter structure will employ a suspended filter membrane fabricated by means of anisotropically etched cavities from the wafer's backside. Pt resistors for heating with a thickness of 500 nm will be patterned using lift-off technique.

MEASUREMENT RESULTS

Characterization of mirror and filter elements is done using the measurement setup shown in Figure 8. Here the emitted spectrum of a tungsten lamp or ASE source (amplified spontaneous emission) is directed perpendicularly onto the device. An optical spectrum

analyzer detects the reflected light. Using a power meter, the filter is aligned with the collimator by adjustating the tip/tilt angles for which maximum intensity is observed. The temperature of the device under test is controlled using a Peltier element.

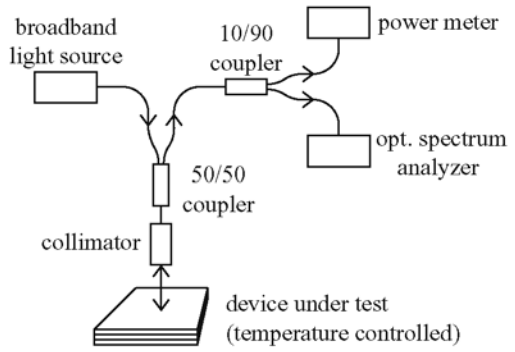

Figure 8. *Measurement setup for characterization of mirror and filter performance.*

Values for maximum reflectivity obtained for the dielectric mirrors are given in Table 3. These were determined using a gold mirror as a reference. Because of the high difference in the refractive index of the two mirror materials, a particularly broad stop-band of several 100 nanometers is generated. It is seen that only three λ/4-stacks are required to reach suitable reflectivity values of about 0.98.

Table 3. *Measured reflectivity data around 1575 nm obtained from dieletric mirrors.*

number of λ/4-stacks	1	2	3	4
max. mirror reflectivity	0.70	0.90	0.97	0.99

Transmission bandwidth and tuning efficiency were also determined for the fabricated filter elements. Figure 9 gives a typical reflectivity spectrum. It can be seen that the filter is highly reflecting for wavelengths above 1200 nm. As desired only one transmission peak appears at a wavelength of 1610 nm.

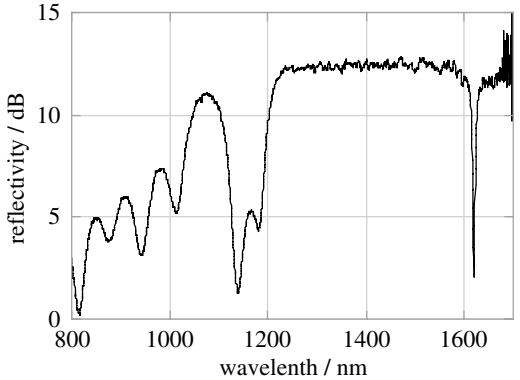

Figure 9. *Spectral response of an optical filter with only one peak around 1600 nm.*

Filter linewidth was determined to be 3.04 nm. Further increase of mirror reflectivity (by increasing the number of λ/4 pairs) as well as optimization of resonator thickness will improve this parameter below 0.5 nm, as required for WDM applications. Due to the thin resonator layer, the free spectral range was greater than the width of the filter's stop-band.

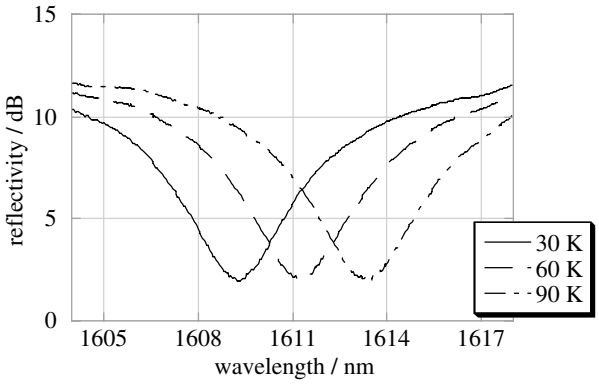

Figure 10. *Thermal tuning of the optical filter, which features a 3dB-bandwidth of 3.04 nm.*

Heating the filter layers increases the optical thickness of the cavity. Thus the filter peak shifts to longer wavelengths (Figure 10). A range of 5.3 nm was covered using external heating with a Peltier element with a temperature difference of 85 K. The tuning efficiency was measured to be 0.071 nm K^{-1}, which is theoretically supported by a model including the thermo-optic coefficient of polycrystalline silicon, $dn/dT = 2.25 \cdot 10^{-4}\ K^{-1}$. The coefficient of thermal expansion of this material is $(dl/dT) / l = 2.6 \cdot 10^{-6}\ K^{-1}$ and can therefore be neglected.

CONCLUSIONS

A new conceopt for a MEMS-based tunable thermo-optical filter has been presented. A linewidth of 3.04 nm was accomplished and the filter peak could be tuned over 5.3 nm through external thermal modulation. Simulation results suggest that this concept enables continuous tuning across either the C- or L-band with a linewidth of about 1 nm. Overall power consumption is expected to be less than 10 mW.

REFERENCES

[1] M. Aziz, et al., "A New and Simple Concept of Tunable Two-Chip Microcavities for Filter Applications in WDM Systems", *IEEE Photonics Technology Letters*, **12**(11), pp. 1522-1524, (2000).

[2] A. Dehé, et al., "III-V Compound semiconductor micromachined actuators for long resonator tunable Fabry-Perot detectors", *Sensors and Actuators A*, **68**, pp.365-371, (1998).

[3] M. Iodice, et al., "Silicon Fabry-Perot filter for WDM systems channels monitoring", *Optics Communications*, **183**, pp. 415-418, (2000).